The American Journal of Pathology, Vol. 171, No. 1, July 2007

DOI: 10.2353/ajpath.2007.061285

Molecular Pathogenesis of Genetic and Inherited Diseases

Neutral Sphingomyelinase (SMPD3) Deficiency Causes a Novel Form of Chondrodysplasia and Dwarfism That Is Rescued by Col2A1-Driven smpd3 Transgene Expression

Wilhelm Stoffel,* Britta Jenke, Barbara Holz, Erika Binczek, Robert Heinz Günter, Jutta Knifka,† Jürgen Koebke,† and Anja Niehoff‡

From the Laboratory of Molecular Neurosciences, Center of Molecular Medicine Cologne, Center of Biochemistry, Cologne; the Center of Anatomy,† Faculty of Medicine, University of Cologne, Cologne; and the Institute of Biomechanics and Orthopaedics,‡ Deutsche Sporthoch-schule Köln, Cologne, Germany*

Neutral sphingomyelinase SMPD3 (nSMase2), a sphingomyelin phosphodiesterase, resides in the Golgi apparatus and is ubiquitously expressed. Gene ablation of smpd3 causes a generalized prolongation of the cell cycle that leads to late embryonic and juvenile hypoplasia because of the SMPD3 deficiency in hypothalamic neurosecretory neurons. We show here that this novel form of combined pituitary hormone deficiency is characterized by the perturbation of the hypothalamus-pituitary growth axis, associated with retarded chondrocyte development and enchondral ossification in the epiphyseal growth plate. To study the contribution by combined pituitary hormone deficiency and by the local SMPD3 deficiency in the epiphyseal growth plate to the skeletal phenotype, we introduced the full-length smpd3 cDNA transgene under the control of the chondrocyte-specific promoter Col2a1. A complete rescue of the *smpd3*$^{-/-}$ mouse from severe short-limbed skeletal dysplasia was achieved. The *smpd3*$^{-/-}$ mouse shares its dwarf and chondrodysplasia phenotype with the most common form of human achondrodysplasia, linked to the fibroblast-growth-factor receptor 3 locus, not linked to deficits in the hypothalamic-pituitary epiphyseal growth plate axis. The rescue of *smpd3 in vivo* has implications for future research into dwarfism and, particularly, growth and development of the skeletal system and for current screening and future treatment of combined dwarfism and chondrodysplasia. ***(Am J Pathol 2007, 171:153–161; DOI: 10.2353/ajpath.2007.061285)***

Sphingomyelinases (SMases) belong to a multigene family of phosphodiesterases.[1] The three well-characterized SMases, sphingomyelin phosphodiesterase SMPD1, SMPD2, and SMPD3, hydrolyze sphingomyelin to ceramides and phosphorylcholine. The acid sphingomyelinase SMPD1 is localized in the endolysosomal compartment, and the neutral SMases SMPD2[2] and SMPD3[1] in the endoplasmic reticulum membranes[3] and in the Golgi apparatus, respectively. Studies *in vitro* and in cell culture suggest important roles of sphingomyelinases, ceramides, and the derived metabolites sphingosine and sphingosine-1-phosphate in intracellular and extracellular signaling in very divergent physiological pathways. However, to date, *in vivo* studies to better clarify the function of SMases are scarce. An ideal approach to pinpoint the function of individual proteins *in vivo* is the knockout of their gene expression by gene targeting in the mouse, as demonstrated by studies on *smpd1*,[4] *smpd2*,[5] and *smpd3*.[6]

We have generated the *smpd3*-null mouse, the phenotype of which is characterized by the impaired secretion of peptide releasing hormones from hypothalamic neurosecretory neurons. Strong perturbation of the hypothalamus-pituitary growth axis and reduction of the number of pituicytes in the anterior lobe of the pituitary in *smpd3*$^{-/-}$ mice led to a novel form of late embryonic-juvenile combined pituitary hormone deficiency. Reduced growth hormone (GH) production and low-serum insulin-like growth factor

Supported by the Center for Molecular Medicine Cologne (CMMC), the Deutsche Forschungsgemeinschaft (Sto32/38-2), and the Gunther and Arina Lauffs Foundation.

Accepted for publication March 15, 2007.

The authors declare that they have no competing financial interests.

Address reprint requests to Wilhelm Stoffel, M.D., Ph.D., University of Cologne, Laboratory of Molecular Neurosciences, Joseph Stelzmannstrasse 52, Cologne, Germany 50931. E-mail: wilhelm.stoffel@uni-koeln.de.

(IGF) 1 concentrations caused a prolongation of the cell cycle in all tissues and led to a generalized hypoplasia. The most striking marker of the *smpd3*$^{-/-}$ mouse is the embryonic and juvenile dwarf phenotype associated with chondrodysplastic bone and joint deformations. We observed a low expression of *smpd3* also in differentiating chondrocytes in the epiphyseal growth zone.

To determine the role of SMPD3 in ossification and longitudinal growth of long bones, we have rescued the *smpd3*$^{-/-}$ mouse from dwarfism and skeletal deformations by introducing the smpd3 cDNA as a transgene into *smpd3*$^{-/-}$ mice. The Col2a1 promoter was used for regulated cell-specific expression of the transgene in the *smpd3*$^{-/-}$ mouse. The smpd3 transgene rescued not only the hypothalamus-pituitary growth axis, normal body weight, and growth but also long bone and joint structure. Our experiments suggest the essential systemic and cell-specific role of SMPD3 in the regulation of normal growth and skeletal development.

Materials and Methods

smpd3$^{-/-}$ and *smpd2/3*$^{-/-}$ Double Knockout Mutant Mouse Lines

The *smpd3*$^{-/-}$ and *smpd2*/3 double knockout mutant mouse lines used in this study have been previously described.[6] Genotypes were assessed by polymerase chain reaction (PCR) and Southern blot hybridization analysis of tail DNA. Homozygous newborn were recognized unambiguously by rhizomelic short, severely deformed fore and hind limbs. The wild-type, *smdp3*$^{+/-}$, and *smpd3*$^{-/-}$ mice used in this study were offspring derived from intercrosses between heterozygous *smpd3*$^{+/-}$ mice on a C57BL/6129Sv.

Smpd3 Transgenic Rescue of the smpd3$^{-/-}$ *Phenotype*

Full-length smpd3 cDNA fused in frame with green fluorescent protein at the 3′ end was ligated blunt-ended into the dephosphorylated *Eco*RV site of the 6.2-kb *col2A1* promoter. The 9-kb transgene sequence was released from the plasmid by *Bss*HII restriction enzyme digestion, subjected to gel electrophoresis, and purified on a Nucleospin column (Macherey & Nagel, Düren, Germany) as a prelude to pronuclear injection into fertilized oocytes from *smpd3*$^{-/-}$ females.

Genotyping of Transgenic smpd3 Mice of Founders and Offspring

The mutated *smpd3* locus (*smpd*3$^{-/-}$) and the transgene of founders and offspring were characterized by PCR using genomic DNA (0.25 to 1 μg). *Smpd3* homozygosity of the founder mice was checked by PCR using primers smpd3 untranslated region 5′ (5′-TGCATGATGAGAGTCTGGGTCCAGACCTGC-3′) annealing to 5′ noncoding sequences external of the targeting construct and smpd3ex1as (5′-CTTGAGAAACAGACCTCCCTTAGAGGCCAG-3′) (expected band size: 3.3 kb). The correct integration of the smpd3-egfp rescue cDNA was confirmed with 5′ forward primer Col2a1proms (5′-TCCTCACCTCCAGCGATATTAGCGCCGCTG-3′) and the smpd3exlas (5′-CTTGAGAAACAGACCTCCCTTAGAGGCCAG-3′) (expected band size: 1.6 kb). The integration of the complete transgene was confirmed with 5′ forward primer Col2a1proms (5′-TCCTCACCTCCAGCGATATTAGCGCCGCTGG-3′) and Col2a1promas (5′-AGCAGGAGGTGTTTGACACAGAATAGCACC-3′) (expected band size: 3.3 kb).

The endogenous col2A1 promoter was amplified by using primer col2A1 prom and Col2A1 rev primer, both annealing to the promoter col2A1. PCR fragments were analyzed in 1.0% agarose gels containing ethidium bromide.

RNA Isolation from Bone and Semiquantitative Reverse Transcription (RT)-PCR

Long bones (femur and tibia) were freed from soft tissues and immediately powderized under liquid nitrogen. Total RNA was isolated for Northern blot analysis by the TRIzol method (Invitrogen, Carlsbad, CA) and poly(A)-mRNA using the Oligotex mRNA Midi Kit (Qiagen, Hilden, Germany) following the manufacturers' recommendations. Quality-controlled RNA was transcribed using mouse leukemia virus reverse transcriptase (Invitrogen). From the total RNA samples isolated by the TRIzol method, between 5 and 10 μg isolated from different tissues were reverse transcribed into cDNA. cDNA aliquots and specific *smpd3* and hypoxanthine-guanine-phosphoribosyl transferase (*hgprt*) sense and antisense primers were used in quantitative PCR amplification. PCR reactions were optimized for each primer pair at 15, 20, 25, and 30 cycles to ensure the linear range and were performed in the presence of 1 μCi of [α-^{32}P]dCTP (1 Ci, 37 GBq). PCR fragments were analyzed on 6% polyacrylamide gels run in sodium borate buffer and then transferred to Whatman filters (Clifton, NJ). Radioactive signals were detected by phosphorimaging, and bands were quantified by densitometric scanning using the IMAGE Quant software (GE Healthcare, Little Chalfont, Buckinghamshire, UK). The signals of *smpd3* were normalized to hgprt cDNA levels.

Protein Analysis of Bone Tissue

Long bones of wild-type and *smpd*3$^{-/-}$ mice were powderized under liquid nitrogen, demineralized by dialysis against 10% acetic acid for 24 hours, and centrifuged at 13,000 rpm, and the sediment was incubated overnight in 0.5 mol/L acetic acid containing 1 mg of pepsin per 20 mg of bone. The turbid solution was cleared by centrifugation at 13,000 rpm for 10 minutes, and the supernatant was used for gradient sodium dodecyl sulfate-polyacrylamide gel electrophoresis (4 to 12%). All steps were performed at 4°C.

Neutral Sphingomyelinase Assay

Neutral SMase (SMPD2 and SMPD3) activity was determined in protein fractions of the Triton X-100 solubilized

100,000 × *g* sediment of the postmitochondrial fraction and acid sphingomyelinase (SMPD1) activity in the sediment of the 12,000 × *g* fraction using N-[$^{14}CH_3$]-sphingomyelin as a substrate.[2,4]

Immunohistochemistry and Histology

Freshly prepared long bones (femur, tibia, and humerus) were fixed in 4% buffered paraformaldehyde overnight and embedded in the methylacrylate polymerization system Technovit 9100 NEU (Heraeus Kulzer, GmbH & Co, Wehrheim, Germany) following the manufacturer's instructions. For immunohistochemistry, 5-μm sections were processed followed by examination under a light microscope. Mouse anti-cartilage oligomeric matrix protein (COMP) and anti-matrilin 3 antibodies were kindly provided by Dr. R. Wagener, Center of Biochemistry, Cologne, Germany. Anti-osteopontin was purchased from Assay Designs, Inc. (Ann Arbor, MI). Cy 3-labeled secondary anti-rabbit antibody was used for immunofluorescence microscopy.

Pituitaries of 18-day-old *wt* and *smpd3*$^{-/-}$ mice were perfused with 4% buffered paraformaldehyde from the left ventricle and embedded, and 5-μm sections were obtained for immunohistochemistry of GH-, thyroid stimulating hormone-, follicle stimulating hormone-, and luteinizing hormone-producing pituicytes. Pituitary hormone antibodies were kindly supplied by Dr. A.F. Parlow, National Hormone and Pituitary Program, National Institute of Diabetes and Digestive and Kidney Diseases, Torrance, CA; anti-GH-releasing hormone was provided by Dr. G. Thordarson, University of California Santa Cruz, Santa Cruz, CA.

Peripheral Quantitative Computed Tomography (pQCT)

Right and left femora of 2-, 7-, and 20-month-old wild-type and *smpd*3$^{-/-}$ mice were scanned by pQCT using the XCT Research M scanner and version 5.50 of the software (Stratec Medizintechnik GmbH, Pforzheim, Germany). For the measurements, isolated bones were placed, with the anterior surface upwards, in a syringe filled with saline solution. After scout view, sections were made at the distal femoral metaphysis (at 15, 17.5, and 20% of total bone length measured from the distal joint line) and at the midshaft (at 50% of total bone length). The voxel size was 500 × 70 × 70 μm. Each slice was analyzed by contour mode 1, peel mode 20 (30%), and cortical mode 1 (710 mg/cm^3). At the femoral metaphysis, total cross-sectional bone area (CSA, mm^2), total bone mineral density (BMD, mg/cm^3), total bone mineral content (BMC, mg), trabecular CSA (Tb.CSA, mm^2), trabecular BMD (Tb.BMD, mg/cm^3), and trabecular BMC (Tb.BMC, mg) were determined as the mean of three slices. At the mid-diaphysis, the cortical area (Ct.CSA, mm^2), the cortical BMD (Ct.BMD, mg/cm^3), the cortical BMC (Ct.BMC, mg), the cortical thickness (Ct.thickness, mm), the periosteal circumference (mm), and the endosteal circumference (mm) were evaluated. Reproducibility of pQCT measurements with the above settings was determined by repeated scans of mouse femora with repositioning. The root-mean square average CV% values were 2.2% for Tb.BMD and 0.7% for Ct.BMD.

Radiography

Anesthesized wild-type and *smp*d3$^{-/-}$ littermates were examined using a bench X-ray unit (HP Cabinet X-ray System-Faxitron series, model 43855A; Hewlett-Packard, McMinnville, OR), with single-side emulsion film (Agfa-Ts Structurix D4DW, NDT System; Grosche, Bottrop, Germany) at 40 kV with exposure times of 25 seconds for young and 50 kV and 48 seconds for adult mice.

Results

Previously, we have generated a *smpd3*$^{-/-}$ mutant mouse using a gene targeting approach. This knockout mouse develops a systemic hypoplasia (dwarfism) due to embryonic and postnatal growth retardation.[6] SMPD3 was seen to play an essential role in Golgi vesicular transport and secretion. Impaired secretion of hypothalamic peptide-releasing hormones by neurosecretory neurons present in the hypothalamus reduces the number of hormone-producing target pituicytes in the anterior lobe of the pituitary gland, particularly of GH, which in turn leads to dysfunctioning of the hypothalamus-pituitary axis in *smpd3*$^{-/-}$ mice. The malfunctioning of this axis causes a novel form of late embryonic-juvenile combined pituitary hormone deficiency.[6]

The most striking markers of the embryonic-juvenile hypoplasia phenotype of the *smpd3*$^{-/-}$ mouse are the retarded longitudinal growth of bones, increased mineralization, and massive malformation of long bones and joints. Here, we investigated the role of *smpd3* expression during the development and growth of the skeletal system and the impact of the loss of *smpd3* expression in the SMPD3-deficient mouse mutant, which was generated by homologous recombination using a targeting construct, in which exon I of the *smpd3* gene was disrupted (Figure 1A). Semiquantitative RT-PCR of multiple tissue RNA demonstrated that s*mpd3* is ubiquitously expressed with highest levels in the central nervous system and the immune system but low levels in bone (Figure 1B). In the mutant mouse, no *smpd3* transcripts were detectable by RT-PCR in total mRNA of long bones (Figure 1C).

Correspondingly, in wild type, neutral SMase (SMPD2 and SMPD3) activity was low in bone protein extracts compared with SMPD1 (Figure 1D). In the *smpd3*$^{-/-}$ mutant mouse, the residual activity was attributed to SMPD2. Note that SMPD2 activity was completely abolished in bone protein extracts of the *smpd2*/*smpd*3 double knockout mutant (Figure 1D).

The early onset of the retarded growth leading to the dwarf phenotype was revealed by comparative X-ray imaging of the skeleton of *smpd3*$^{-/-}$ embryos of age e16, p2, and p18, as well as juvenile and 18-month-old adult mutant mice. Severe short-limb dwarfism with pronounced joint deformation was observed during the early

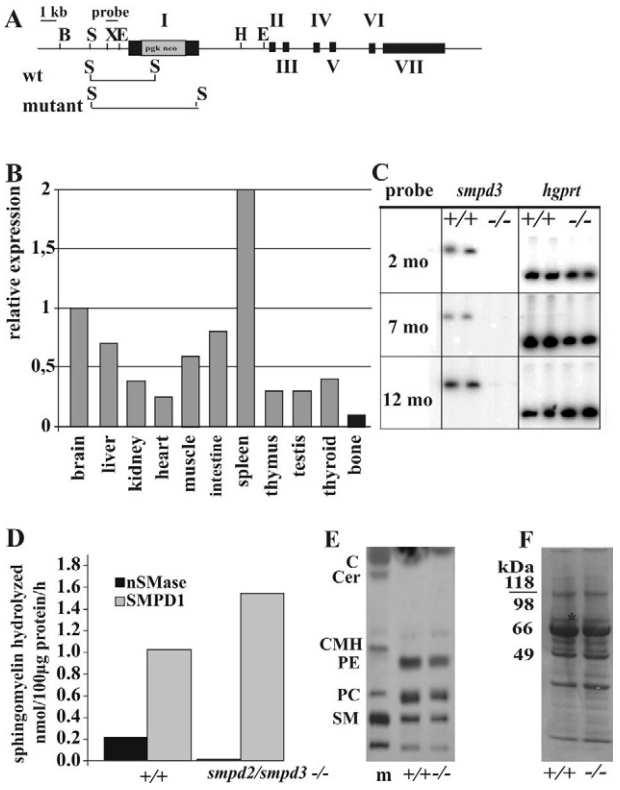

Figure 1. Deletion of *smdp3* expression, neutral and acid sphingomyelinase activity in *smpd3*$^{-/-}$ and *smpd2*/*smpd3* double mutant lipid, and protein patterns in *smpd3*$^{-/-}$ bone. **A:** Targeted deletion of the *smpd3* gene locus by disruption of exon I of *smpd3*. B, *Bam*HI; E, *Eco*RI; H, *Hind*III S, *Sst*I; X, *Xho*I. **B:** Multitissue expression of *smpd3*. Semiquantitative RT-PCR of total RNA of brain, liver, heart, kidney, muscle, intestine, spleen, testes, thymus, thyroid, and bone. **C:** Semiquantitative RT-PCR of bone total RNA extracted from 2-, 7-, and 12-month-old wt and *smpd3*$^{-/-}$ mice. **D:** Combined SMPD2 and 3 (nSMase) enzyme activity is low in bone protein extracts of wild-type mouse but lacking in bone protein extracts of *smpd3*$^{-/-}$ mice. SMPD1 is abundant in bone of control as well as *smpd3*$^{-/-}$ and *smpd2/smpd3*$^{-/-}$ mice. **E:** Lipid analysis of long bone (femur, tibia, and humerus) of control and *smpd3*$^{-/-}$ mice reveals no difference in the complex phospho- and sphingolipid profiles. **F:** Protein profiles in extracts taken from long bones of control and *smpd3*$^{-/-}$ mice are similar. Bar indicates the position of the collagen α_1 I band.

postnatal growth phase when pressure and traction are exerted on femur, tibia, humerus, and the thoracic and lumbar vertebra (Figure 2, A–F). The articular ends of femur, tibia, and humerus are bossed, and elbow and knee joints are restricted in rotation and extension. The lateral view clearly shows kyphosis in the thoracolumbar area. *Smpd3*$^{-/-}$ mice also have a narrow long trunk and a disproportionately large head (Figure 2A). Moreover, X-ray imaging indicated enhanced calcification of ossified bones of *smpd3*$^{-/-}$ mice beyond 2 months of age, which was quantified here by pQCT (Figure 2, E and H). Note that in the *smpd3*$^{-/-}$ mouse mutant, incisors were normally formed, and no fractures or callus formation were observed.

Therefore, to compare BMD (mg/cm^3), pQCT was used for the femur of control and *smpd3*$^{-/-}$ mice at age 2, 7, and 20 months (Figure 2H). BMD was higher at the metaphysis of *smpd3*$^{-/-}$ mice than in control: 543 ± 15 versus 426 ± 6 (2 months), 535 ± 14 versus 428 ± 13 (7 months), and 546 ± 2 versus 354 ± 1 (20 months), and likewise ctBMD at the mid-diaphysis in agreement with the X-ray data. Therefore a lack of SMPD3 seems not to affect mineralization of bone. Further, the periosteal and endosteal circumferences appear to be similar (Figure 2G).

Because sphingomyelin metabolism and storage in the SMPD1-deficient Niemann-Pick mouse are known to be severely affected,[4] we performed lipid (sphingomyelin, sphingosine, and ceramide) analyses of long bones of control and *smpd3*$^{-/-}$ mice. Examination of the total lipid profiles revealed no storage of sphingomyelin in *smpd3*$^{-/-}$ mice. Unlike the SMPD1-deficient mouse,[4] macrophages of the *smpd3*$^{-/-}$ bone marrow showed no sphingomyelin accumulation, and the ceramide concentration also remained unchanged. The absence of sphingomyelin storage in other reticuloendothelial tissues has been shown previously.[6] Therefore, we conclude that nSMase deficiency has no impact on the lipid composition in bones in general and on sphingomyelin and ceramide metabolism and storage in particular.

We next studied the organization of the epiphyseal growth plate of the proximal tibia of wild-type and *smpd3*$^{-/-}$ mice by immunohistochemistry. The proximal tibia of *smpd3*$^{-/-}$ mice showed a narrow and disorganized growth zone, irregular columnization of cartilage with short rows of small cells, and reduced hypertrophic cells columns. Primary trabeculae were thick, irregularly arranged, and scarcely calcified. SPMD3, collagen, and three noncollagenous proteins abundant in the cartilage extracellular matrix of the epiphyseal growth plate, COMP,[7–9] matrilin 3,[10,11] and osteopontin[12] were also studied. In wild-type p20 mice, COMP is uniformly distributed throughout the interterritorial extracellular matrix of cartilage. However, even at p20 *smpd3*$^{-/-}$ mice, COMP immunostaining of cartilage was still restricted to the immediate pericellular matrix of the chondrocytes similar to the COMP distribution in human fetal cartilage.[9] Large longitudinally oriented and tightly aligned islets of cartilage extend into the ossification zone of long bones in age- and gender-matched control mice, whereas in the *smpd3*$^{-/-}$ mutant, layers of COMP and matrilin-positive small and irregularly shaped chondrocytes form a sharp boundary toward the ossification zone (Figure 3, A and B). Osteopontin-reactive material surrounded large chondrocytes ordered in columns in the growth plate of control mice, whereas in the *smpd3*$^{-/-}$ mouse, irregularly packed small chondrocytes were covered with osteopontin (Figure 3C). Severe disorganization of collagen bundles between chondrocytes was also observed in the *smpd3*$^{-/-}$ mutant mouse (Figure 3E). These data indicate that the delayed maturation of chondroblasts together with an abnormal extracellular arrangement of noncollagenous proteins and of collagen in the extracellular matrix of cartilage during late embryonic and juvenile development delays the longitudinal growth of long bones and leads to diaphyseal and joint deformations. Smpd3 is also expressed locally in chondrocytes in the epiphyseal growth zone (Figure 3D). Therefore, SMPD3 deficiency in differen-

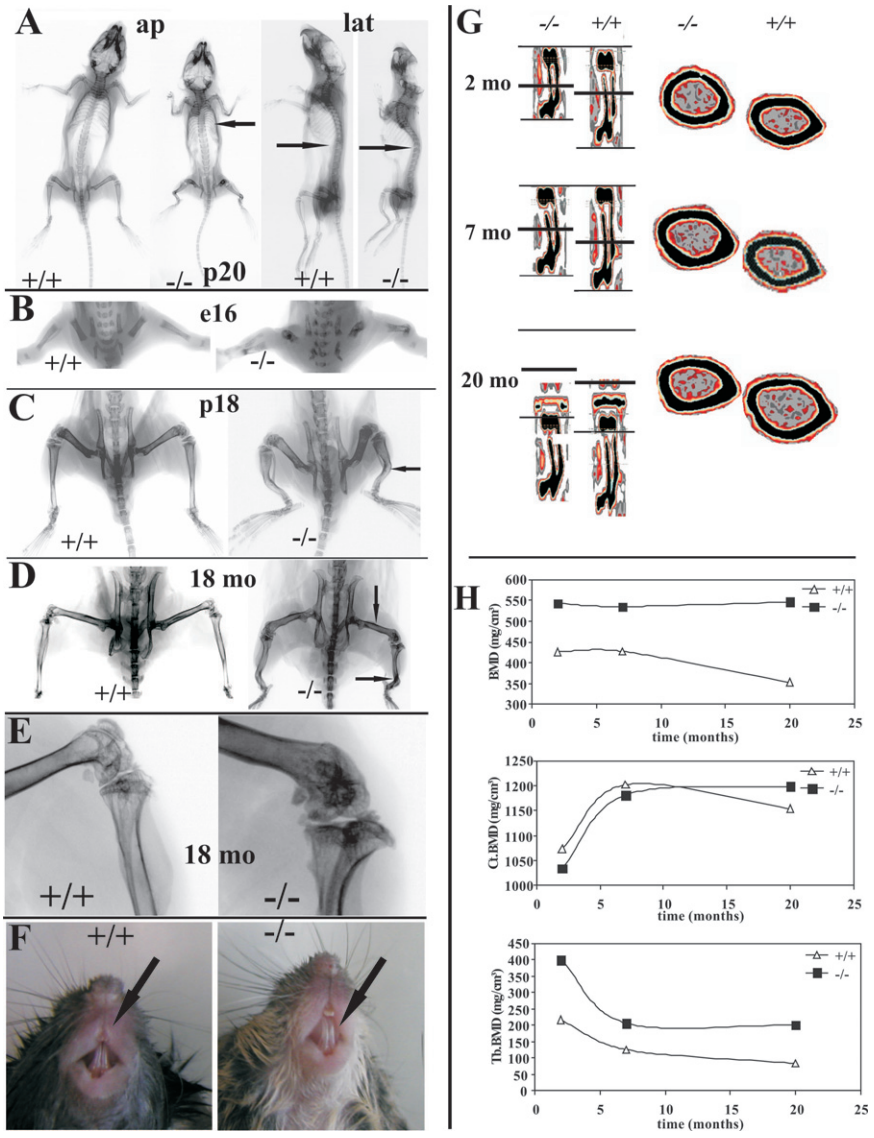

Figure 2. Short-limbed dwarfism and severe skeletal deformation in *smpd3*$^{-/-}$ mice (**A–F**). **A:** Anteroposterior X-ray imaging reveals rhizomelic long bones and a cage-shaped thorax (**arrow**) in p20 *smpd3*$^{-/-}$ mice. **B:** Skeletal phenotype observed during late embryonic development (e16). **C:** Short stature and deformation of femora, tibiae, and humeri are fully developed in juvenile mice (p18) and (**D**) in adult (18 mo) *smpd3*$^{-/-}$ mice and are maintained throughout the life span (**E**). No fractures or callus formation were observed. Elbow and knee joints show severe deformations with exostoses (**arrows**). **F:** Normal dentinogenesis of maxillary and mandibular incissors. Note that the same level of X-ray emission was used for all presented X-rays here. pQCT reveals unimpaired mineralization and ossification in the adult *smpd3*$^{-/-}$ mouse (**G** and **H**). **G:** Isolated right and left femora of 2-, 7-, and 20-month-old *wt* and *smpd3*$^{-/-}$ mice were scanned using pQCT. Sections were made at the distal femoral metaphyses (at 15, 17.5, and 20% of total bone length measured from the distal joint line) and at the midshaft (at 50% of total bone length) (**bars**). **H:** Quantification of total BMD and cortical and trabecular BMD over a period of 20 months. At the femoral metaphysis, total CSA (mm^2), total BMD (mg/cm^3), total BMC (mg/cm^3), trabecular CSA (Tb.CSA, mm^2), trabecular BMD (Tb.BMD, mg/cm^3), and trabecular BMC (Tb.BMC, mg) were determined as the mean of three slices. At the mid-diaphysis, the cortical CSA (Ct.CSA, mm^2), the cortical BMD (Ct.BMD, mg/cm^3), the cortical BMC (Ct.BMC, mg), the cortical thickness (Ct.thickness, mm), the periosteal circumference (mm), and the endosteal circumference (mm) were evaluated. Comparison of metaphyseal BMD (mg/cm^3), cortical BMD (Ct.BMD, mg/cm^3), and trabecular BMD (Tb.BMD, mg/cm^3) of 2-, 7-, and 20-month-old *wt* and *smpd3*$^{-/-}$ mice is shown.

tiating chondrocytes might contribute to the skeletal phenotype. In *smpd3*$^{-/-}$ mice, bones are deformed, but no fractures occur, and mineralization is normal. We did not observe any SMPD3-immunoreactive protein in the growth plate and the primary ossification center or the calcified shaft of long bones of *smpd3*$^{-/-}$ mice (Figure 3D).

Our biochemical, cell biological, and morphological results suggest that the disturbed growth and the deformation of long bones of the *smpd3*$^{-/-}$ mouse might have its dominant origin in the dysfunction of the hypothalamus-pituitary-epiphyseal growth plate axis but less in local SMPD deficiency in chondrocytes of the growth plate. Here, we confirm the role of SMPD3 in the development of the severe skeletal phenotype by a rescue experiment, in which pronuclear injection of smpd3 cDNA as transgene abolished dwarfism and skeletal deformations in the *smpd3*$^{-/-}$ mouse.

The promoter of the *Col2A1* gene is known to induce chondrocyte-specific expression. Therefore, high-level expression would be expected in cartilaginous tissues although low-level expression has also been observed in extraskeletal locations, such as the developing brain[13,14].

To this end, full-length smpd3 cDNA was fused with enhanced green fluorescent protein and inserted 3′ to the *Col2a1* promoter.[14] The Col2a1-smpd3-egfp gene construct carried the 5′ sequences of the mouse type II collagen promoter as described before[14] (Figure 4A). A 9-kb *Bsst*II fragment free of vector sequences was used for pronuclear microinjection into fertilized *smpd3*$^{-/-}$ oocytes. The mutated *smpd3* locus and the transgene of founders and offspring were characterized by PCR (Figure 4, B–E). The primers and their sequences are listed under Materials and Methods. A total of four independent founders were obtained, and the copy number of the transgene determined by semiquantitative PCR as described under Materials and Methods. Founders carried copy numbers between three and six. Founder 5, with six copies of the smpd3 transgene, was used to establish a stable transgenic

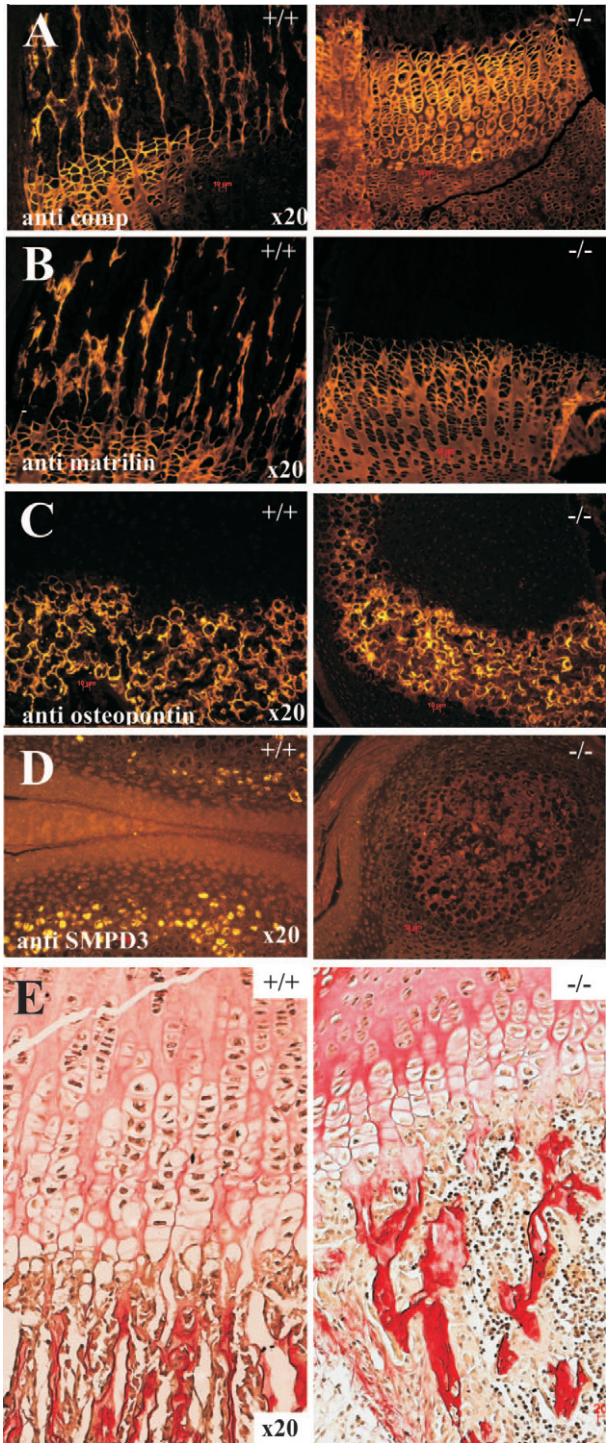

Figure 3. Retarded transition of proliferative into hypertrophic chondrocytes and ossified trabeculae in the tibial growth plate of p20 *smpd3*$^{-/-}$ mouse. **A–E:** Immunohistochemistry of chondrocytes and extracellular matrix proteins in sections (5 μ) of the tibial epiphyseal growth plate of undecalcified tibia of *smpd3*$^{-/-}$ mice using (**A**) anti-COMP and (**B**) anti-matrilin 3 antibodies. Left: Control (+/+); lane: *smpd3*$^{-/-}$ mutant (−/−). Oriented columns of ossifying trabecular structures in the growth plate of control are missing in the mutant. **C:** Anti-osteopontin visualizes the small and irregularly shaped immature chondrocytes in the mutant. **D:** Anti-SMPD3 antibodies indicate the faint expression of smpd3 in epiphyseal chondrocytes of control mice, which are missing in the *smpd3*$^{-/-}$ mutant. **E:** Picrosirius red staining reveals the irregular orientation of collagen in the growth plate of *smpd3*$^{-/-}$ mice. Anti-SMPD3 antibodies stained the lacunae of hyaline chondrocytes, which surround the secondary epiphyseal ossification center in a rim-like arrangement.

line. In the *smpd3*$^{-/-}$ rescued mouse, the smpd3 transgene was expressed in most organs, once again strongest in brain, but also in bone. Semiquantitative RT-PCR indicated ubiquitous *smpd3* expression, strongest in brain, jejunum, kidney, thymus, and bones. (Figure 4F). Comparative immunohistochemistry of the hormone-secreting pituicytes in the anterior pituitary lobe of control wt, *smpd3*$^{-/-}$, and rescued *smpd3*$^{-/-}$ mice (age p15), using GH, thyroid-stimulating hormone, follicle-stimulating hormone, and luteinizing hormone antibodies, documented the return of the anterior pituitary secretory function and demonstrated that, secondary to the rescue of smpd3 expression, a high level of correction of the combined pituitary hormone deficiency had occurred (Figure 5).

The extensive return of the anterior pituitary hormone secretion is the dominant driving force of the rescue, which completely restored body size and weight and the time point of fertility. Despite the "chondrocyte-specific" promoter driving the smpd3 expression, smpd3 in chondrocytes remains low as in the wild type.

X-ray imaging revealed a regular morphology of long bones of fore and hind legs in the *smpd3*$^{-/-}$ rescued mouse (Figure 4, G–J). The development and organization of epiphyseal growth plates were normalized. Moreover, the smpd3 transgene restored the regular morphology of the epiphyseal growth plate (Figure 4, K–N). Regulated expression of the transgene under the control of the Col2a1 promoter not only rescued normal longitudinal growth and ossification of long bones, as well as abolishing chondrodysplastic deformations, but also rescued normal systemic growth. Thus, our rescue experiments establish the essential systemic and cell-specific role of SMPD3 in the regulation of skeletal development as well as normal growth. Taken together, the present study provides substantial evidence for an important role of SMPD3 in normal chondrocyte differentiation and enchondral ossification in the growth plate of long bones during late embryonic and postnatal and juvenile development, essential for regular longitudinal growth.

Malfunctioning of the hypothalamus-pituitary axis in *smpd3*-null mice perturbs the pituitary-epiphyseal growth plate axis because of the low GH production by the reduced number of somatotrophic pituicytes.[8] GH controls chondrocyte proliferation and IGF1 chondrocyte differentiation.[15] GH exerts indirect effects via IGF, but the two hormones, GH and IGF1, also exert direct local effects on epiphyseal chondroblasts in the germinal zone, and, in addition, IGF1 enhances the development to hypertrophic chondrocytes.[16,17]

Discussion

Our results suggest that hypothalamus-induced combined pituitary hormone deficiency causes late embryonic and postnatal growth retardation of the *smpd3*$^{-/-}$ mouse, which is particularly manifested in the retarded maturation of chondrocytes and ossification in the epiphyseal growth plate, leading to dwarfism and severe skel-

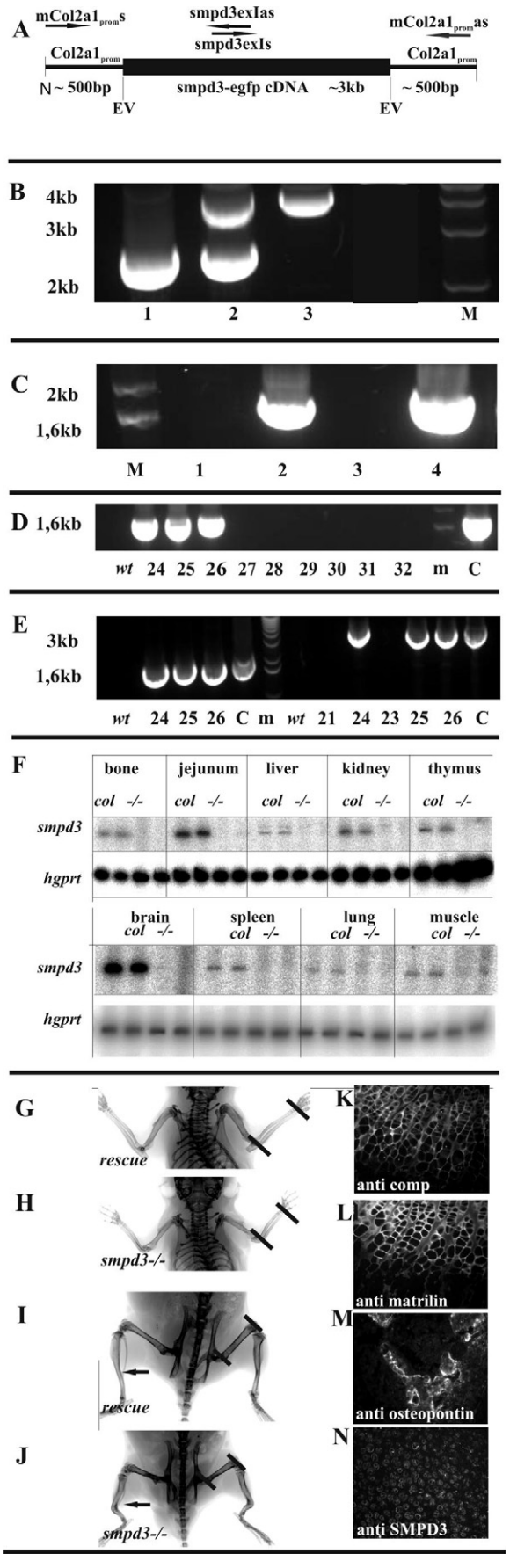

Figure 4. Rescue of *smpd3* expression in the *smpd3*$^{-/-}$ mouse by smpd3-egfp cDNA under the control of the col2A1 promoter. **A:** Construct of the transgene with location of oligonucleotide primers applied in genotyping by PCR of genomic DNA of founder and offspring. **B:** Proof of *smpd3*$^{-/-}$ homozygosity of Col-smpd3-rescue mice, using primers smpd3 untranslated region 5′ and smpd3ex1as. 1, wt; 2, heterozygote; and 3, Col mouse. **C:** Col2a1prom-smpd3-rescue founder mouse 5. 1, wt (mCol2a1 proms/smpd3exIas). 2, Col mouse (mCol2a1proms/smpd3exIas). 3, wt. 4, Col mouse (smpd3exIIs/mCol2a1 prom as). **D:** Genotyping of littermates; primers mCol2a1proms/smpd3exIas. **E:** Offspring of founder mouse 5. Primer pairs: left, smpd3exII s/mCol2a1promas; right, mCol2a1proms/mCol2a1promas; C, positive control, plasmid construct. **F:** Semiquantitative RT-PCR of multitissue mRNA of transgenic *smpd3*$^{-/-}$ mice (col) and *smpd3*$^{-/-}$ homozygous mice (−/−). The col 2A1-promoter causes ubiquitous expression of *smpd3*, strongest in brain, followed by jejunum, kidney, and bone. Hgprt mRNA was used as marker for internal standardization. Primer sequences are listed under Materials and Methods. **G–J:** X-ray images of long bones of founder rescue mouse 5 and *smpd3*$^{-/-}$ siblings. Fore legs of rescued *smpd3*$^{-/-}$ founder and *smpd3*$^{-/-}$ mutant mice. **I** and **J:** Hind legs of rescued *smpd3*$^{-/-}$ founder and *smpd3*$^{-/-}$ mutant mice. Note the deformations of the mutant tibia (**arrow**) are missing. The length of radius, ulna, and femora in the two genotypes are marked by **lines**. **K–N:** Rescue of regular chondrocyte development. Immunohistochemistry of chondrocytes and extracellular matrix of epiphyseal growth plate of tibia of *smpd3*$^{-/-}$ mice expressing the col2A1$_{prom}$-smpd3-egfp transgene. **K:** Anti-COMP. **L:** Anti-matrilin 3; maturating chondrocytes are oriented in trabecular structure. **M:** Ossified trabeculae are stained with anti-osteopontin antibodies. **N:** SMPD3 is expressed in all chondrocytes of the growth plate.

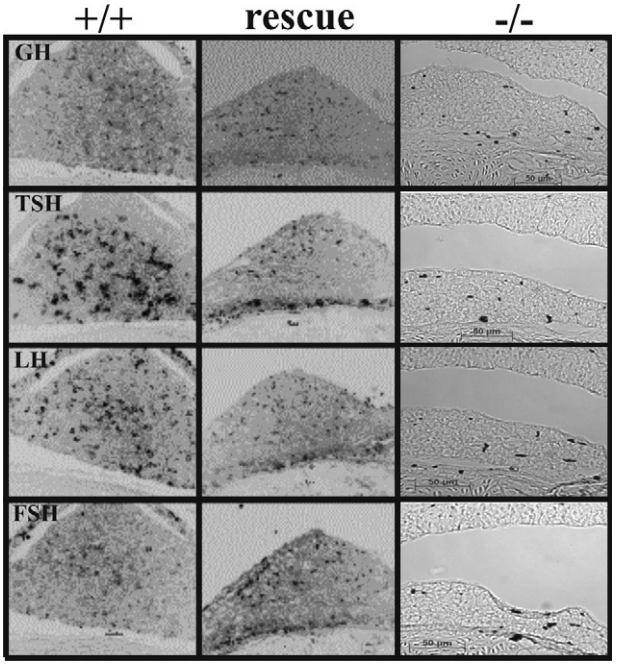

Figure 5. Rescue of the hypothalamus pituitary growth axis by transgenic rescue with smpd3 under the control of Col1 promoter. Immunohistochemistry of cross sections of pituitary of wt control (+/+), smpd3$^{-/-}$ mutant expressing the smpd3 transgene (Col2a1prom-smpd3 rescue mouse) (rescue), and smpd3$^{-/-}$ mutant (−/−). Anti-GH, -TSH (thyroid-stimulating hormone), -LH (luteinizing hormone), and -FSH (follicle-stimulating hormone) antibodies were applied to 5-μm paraffin sections as described before.[6]

etal chondrodysplasia. The *smpd3*$^{-/-}$ mutation is therefore not a primary disorder of cartilage and bone development. The phenotype of the *smpd3*$^{-/-}$ mouse mimics that of human chondrodysplasia, a genetic disorder with great heterogeneity within the clinical syndrome. One form is achondroplasia, inherited as a primary disorder of bone or cartilage in autosomal dominant fashion. This most common form of short-limb dwarfism with de-

layed enchondral ossification has been assigned to the fibroblast growth factor receptor 3 locus.[18–20]

The *smdp*3$^{-/-}$ mouse also differs significantly from the "fro" (fragilitas ossium) mouse, which was isolated from a randomly bred stock of mice generated by chemical mutagenesis with the mutagen Tris(1-aziridinyl) phosphine-sulfine. fro is an autosomal recessive mutation with high lethality assigned to the deletion of a 1.5-Mb chromosomal segment in the midpart of mouse chromosome 8.[19] Recently, intron 8 and most of exon 9 of the *smpd3* gene were reported to be part of this deletion.[20]

The fro phenotype is characterized by osteoporosis due to enhanced osteoclast activity, multiple fractures of the long bones and ribs, diaphyseal deformations, thin cortices, calluses, short stature, brittle teeth, and reduced osteoblasts. fro$^{-/-}$ mutant mice appear to have normal cartilage growth despite exhibiting hypomineralization. Loss of local SMPD3 activity and defective sphingomyelin hydrolysis, as well as disruption of the ceramide pathway including sphingosine-1 phosphate, have been proposed to affect bone mineralization and lead to bone fragility.[20] Because the fro/fro mouse shares symptoms with a severe, recessive form of human osteogenesis imperfecta, it has been proposed as a mouse mutant model for this disease.[19–23] The fro and *smpd3*$^{-/-}$ mutant mice described here have contrasting phenotypes. Maturation of chondrocytes in the epiphyseal growth plate of our *smpd3*$^{-/-}$ mice is severely perturbed, mineralization of long bones of juvenile *smpd3*$^{-/-}$ mice is normal and, in adult null mice, significantly stronger than in control animals. Therefore, these hallmarks of the *smpd3*$^{-/-}$ mutant mouse offer phenotypic markers that differ from those for the fro$^{-/-}$ mouse. Ceramide and sphingosine-1 phosphate, two metabolites of sphingomyelin catabolism missing in the fro$^{-/-}$ mouse, have been proposed as signaling molecules for the hypermineralization of the osteogenesis imperfecta phenotype. However, analytical data of bone lipid extracts of the fro$^{-/-}$ mutant are currently not available. Interestingly, the lipid composition (including sphingomyelin, ceramide, and sphingosine) in bone extracts of control, *smpd3*$^{-/-}$, and the double mutant *smpd2/smpd3*$^{-/-}$ mice, completely devoid of neutral sphingomyelinase activity, was identical. The contrasting phenotypes of the fro$^{-/-}$ and *smpd*3$^{-/-}$ mutant mice can hardly be explained by differences in the genetic background of the two mouse lines. The background of the *smpd*3$^{-/-}$ mouse is C57BL/6x129Sv, which has been backcrossed for more than 10 generations into C57BL/6.

The question therefore arises as to whether the *smpd*3 deletion in the fro$^{-/-}$ mouse induced by chemical mutagenesis is of a random nature and only one symptom, and that the manifesting phenotype is not due specifically to *smpd*3 deletion, but rather to the whole gamut of point mutations, insertions, deletions, and rearrangements in the genome, superimposing the molecular pathology of the *smpd3* deletion by a variety of additional unknown molecular events. In other words, this observation may be due to complex mutagenesis masking the specific effect of deletion of *smpd3* alone. This hypothesis can only be clarified by a broad and comprehensive genetic analysis of the fro$^{-/-}$ mouse mutant.

References

1. Hofmann K, Tomiuk S, Wolff G, Stoffel W: Cloning and characterization of the mammalian brain-specific, Mg2+-dependent neutral sphingomyelinase. Proc Natl Acad Sci USA 2000, 97: 5895–5900
2. Tomiuk S, Hofmann K, Nix M, Zumbansen M, Stoffel W: Cloned mammalian neutral sphingomyelinase: functions in sphingolipid signaling? Proc Natl Acad Sci USA 1998, 95:3638–3643
3. Tomiuk S, Zumbansen M, Stoffel W: Characterization and subcellular localization of murine and human magnesium-dependent neutral sphingomyelinase. J Biol Chem 2000, 275:5710–5717
4. Otterbach B, Stoffel W: Acid sphingomyelinase-deficient mice mimic the neurovisceral form of human lysosomal storage disease (Niemann-Pick disease). Cell 1995, 81:1053–1061
5. Zumbansen M, Stoffel W: Neutral sphingomyelinase 1 deficiency in the mouse causes no lipid storage disease. Mol Cell Biol 2002, 22:3633–3638
6. Stoffel W, Jenke B, Block B, Zumbansen M, Koebke J: Neutral sphingomyelinase 2 (smpd3) in the control of postnatal growth and development. Proc Natl Acad Sci USA 2005, 102:4554–4559
7. Oldberg A, Antonsson P, Lindblom K, Heinegard D: COMP (cartilage oligomeric matrix protein) is structurally related to the thrombospondins. J Biol Chem 1992, 267:22346–22350
8. Newton G, Weremowicz S, Morton CC, Copeland NG, Gilbert DJ, Jenkins NA, Lawler J: Characterization of human and mouse cartilage oligomeric matrix protein. Genomics 1994, 24:435–439
9. DiCesare P, Hauser N, Lehman D, Pasumarti S, Paulsson M: Cartilage oligomeric matrix protein (COMP) is an abundant component of tendon. FEBS Lett 1994, 354:237–240
10. Wagener R, Kobbe B, Paulsson M: Primary structure of matrilin-3, a new member of a family of extracellular matrix proteins related to cartilage matrix protein (matrilin-1) and von Willebrand factor. FEBS Lett 1997, 413:129–134
11. Ko Y, Kobbe B, Nicolae C, Miosge N, Paulsson M, Wagener R, Aszodi A: Matrilin-3 is dispensable for mouse skeletal growth and development. Mol Cell Biol 2004, 24:1691–1699
12. Reinholt FP, Hultenby K, Oldberg A, Heinegard D: Osteopontin—a possible anchor of osteoclasts to bone. Proc Natl Acad Sci USA 1990, 87:4473–4475
13. Metsäranta M, Garofalo S, Smith C, Niederreither K, de Crombrugghe B, Vuorio E: Developmental expression of a type II collagen/beta-galactosidase fusion gene in transgenic mice. Dev Dyn 1995, 204:202–210
14. Sakai K, Hiripi L, Glumoff V, Brandau O, Eerola R, Vuorio E, Bosze Z, Fassler R, Aszodi A: Stage-and tissue-specific expression of a Col2a1-Cre fusion gene in transgenic mice. Matrix Biol 2001, 19:761–767
15. Le Roith D, Bondy C, Yakar S, Liu JL, Butler A: The somatomedin hypothesis: 2001. Endocr Rev 2001, 22:53–74
16. Wang J, Zhou J, Powell-Braxton L, Bondy C: Effects of Igf1 gene deletion on postnatal growth patterns. Endocrinology 1999, 140:3391–3394
17. Hunziker EB, Wagner J, Zapf J: Differential effects of insulin-like growth factor I and growth hormone on developmental stages of rat growth plate chondrocytes in vivo. J Clin Invest 1994, 93:1078–1086
18. Rousseau F, Bonaventure J, Legeai-Mallet L, Pelet A, Rozet JM, Maroteaux P, Le Merrer M, Munnich A: Mutations in the gene encoding fibroblast growth factor receptor-3 in achondroplasia. Nature 1994, 371:252–254
19. Aubin I, Poirier C, Muriel MP, Stanescu V, Guenet JL: Positional cloning of the mouse mutation fragilitas ossium (fro). The 16th International Mouse Genome Conference San Antonio, TX; 2002 November 17–20, Poster 139
20. Aubin I, Adams CP, Opsahl S, Septier D, Bishop CE, Auge N, Salvayre R, Negre-Salvayre A, Goldberg M, Guenet JL, Poirier C: A deletion in the gene encoding sphingomyelin phosphodiesterase 3

(Smpd3) results in osteogenesis and dentinogenesis imperfecta in the mouse. Nat Genet 2005, 37:803–805
21. Guenet JL, Stanescu R, Maroteaux P, Stanescu V: Fragilitas ossium: a new autosomal recessive mutation in the mouse. J Hered 1981, 72:440–441
22. Muriel MP, Bonaventure J, Stanescu R, Maroteaux P, Guenet JL, Stanescu V: Morphological and biochemical studies of a mouse mutant (fro/fro) with bone fragility. Bone 1991, 12:241–248
23. Sillence DO, Ritchie HE, Dibbayawan T, Eteson D, Brown K: Fragilitas ossium (fro/fro) in the mouse: a model for a recessively inherited type of osteogenesis imperfecta. Am J Med Genet 1993, 45:276–283